

# Saturation of the Anomalous Hall Effect in Critically Disordered Ultra-thin $\text{CNi}_3$ Films

Y. M. Xiong, P. W. Adams

*Department of Physics and Astronomy, Louisiana State University, Baton Rouge, LA 70803-4001, USA*

G. Catelani

*Department of Physics, Yale University, 217 Prospect Street, New Haven, CT 06520, USA*

(Dated: May 24, 2022)

We demonstrate that a distinct *high-disorder* anomalous Hall effect phase emerges at the correlated insulator threshold of ultra-thin, amorphous, ferromagnetic  $\text{CNi}_3$  films. In the weak localization regime, where the sheet conductance  $G \gg e^2/h$ , the anomalous Hall resistance of the films increases with increasing disorder and the Hall conductance scales as  $G_{xy} \propto G^\varphi$  with  $\varphi = 1.6$ . However, at sufficiently high disorder the system begins to enter the 2D correlated insulator regime, at which point the Hall resistance  $R_{xy}$  abruptly saturates and the scaling exponent becomes  $\varphi = 2$ . Tunneling measurements show that the saturation behavior is commensurate with the emergence of the 2D Coulomb gap, suggesting that *e-e* interactions mediate the high-disorder phase.

PACS numbers: 73.50.Jt, 73.20.Fz, 75.47.-m

One of the most far-reaching goals in condensed matter physics is to develop a comprehensive understanding of how electron-electron (*e-e*) interactions, and their attendant correlations, affect the electronic properties of two dimensional (2D) systems. It is now well known that reduced dimensionality often induces profound changes in the electronic behavior of materials, particularly in the presence of disorder. Indeed, interesting manifestations of electron correlation effects have been reported in a wide variety of 2D systems, including homogeneously disordered metal films [1, 2], thin film superconductors [3], and two dimensional electron gasses in semiconducting heterojunctions [4], to name a few. In the present Letter, we show that the anomalous Hall effect (AHE) [5] also offers a compelling stage from which to study the manifestations of disorder-enhanced quantum correlations but from a perspective in which spin-dependent scattering processes are important. In addition, because the effect arises from both magnetic scattering and intrinsic band mechanisms, it remains a topic of current interest, with relevance to the burgeoning field of spintronics.

The AHE is characterized by the appearance of a spontaneous Hall resistance in magnetic materials and is usually parameterized by the empirical relation [6–8],

$$R_H = V_H/I = (R_o B + R_e \mu_0 M)/t, \quad (1)$$

where  $R_H$  is the Hall resistance,  $V_H$  is the Hall voltage,  $I$  is the longitudinal current,  $R_o$  is the ordinary Hall coefficient,  $R_e$  is the anomalous (extraordinary) Hall coefficient,  $M$  is the magnetization, and  $t$  is the film thickness. The term proportional to  $M$  in Eq. 1 produces the anomalous Hall voltage and, in transition metal ferromagnetic films, it is usually orders of magnitude larger than the ordinary Hall term. The robustness of the AHE signal offers one a potentially important probe of localization effects as manifest in the three predominant AHE channels: *intrinsic inter-band scattering*, *skew scattering*, and *side-jump scattering* [5]. The theoretical treatment of the AHE has a long and contentious history, but in recent years there has been a significant interest in how disorder-enhanced quantum correlations affect the low-temperature behavior of the AHE and, in particular, how such corrections are related to the well-established weak-localization corrections to the longitudinal transport [1]. This remains an open issue, particularly in the regime of moderate to strong disorder [6, 9–11]. In this Letter, we present a study of the low-temperature anomalous Hall effect as a function of the sheet resistance of homogeneously disordered  $\text{CNi}_3$  films. Using magnetotransport and tunneling density of states (DOS) measurements we show that, although the magnitude of the AHE initially increases with increasing disorder, it eventually saturates and becomes disorder independent once the film resistance reaches values that are of the order of the quantum resistance  $R_Q = h/e^2$ . Spin-resolved tunneling DOS spectra show that the conduction electron polarization of the films remains constant throughout the region of study, and that the saturation behavior is associated with a rapid attenuation of states near the Fermi energy as  $R \rightarrow R_Q$ .

It is now well-established that, in the weak-localization limit, *e-e* interactions produce a perturbative logarithmic depletion of states near the Fermi energy. As the sheet resistance of the film is increased the magnitude of the depletion region grows. Finally, as one approaches  $R_Q$  the effects of *e-e* correlations on the DOS are no longer perturbative and, in fact, a correlation gap begins to open in the DOS spectrum [12]. In this regime the transport usually exhibits a modified variable-range hopping form, and macroscopic phases that are nominally robust to disorder begin to become

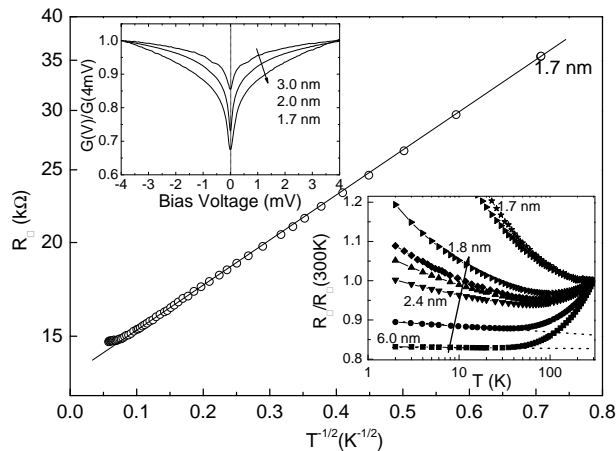


FIG. 1: The main panel shows a semi-log plot of the sheet resistance of 1.7 nm-thick  $\text{CNi}_3$  film as a function of  $T^{-1/2}$ . The solid line is a fit to Eq. 2. Upper inset: Electron tunneling conductance at 100 mK as a function of bias voltage for three  $\text{CNi}_3$  films of varying thickness. Lower inset: The normalized sheet resistance as a function of  $\ln T$  for  $\text{CNi}_3$  films of thicknesses 6.0, 4.0, 2.4, 2.1, 1.9, 1.8, 1.75, and 1.7 nm.

affected. For instance, if the system is a superconductor, then the superconducting phase is usually lost as  $R \rightarrow h/4e^2$  [13].

Altshuler and coworkers [2] first showed that the ordinary Hall conductivity exhibits coherent scattering corrections but no  $e$ - $e$  interaction corrections. Extensions of this work to the AHE also predicted that there would be no interaction corrections to the AHE conductivity in the weak disorder limit; which was, indeed, verified in measurements of quenched condensed Fe films in the early 1990's [6, 9]. However, more recent measurements on Fe/Si multilayers and high-resistance Fe films have suggested that disorder-enhanced  $e$ - $e$  correlations are reflected in the scaling behavior of the AHE conductivity [10, 11]. Though it is now evident that quantum correlations emerge as the disorder is increased beyond the weak limit, the current state of understanding does not shed much light on the influences dimensionality, microscopic morphology, and scattering mechanisms have on the manifestations of a correlation-modified AHE. Furthermore, previous studies have primarily reported scaling behavior in which the film resistance was varied by changing the temperature. Here, in contrast, we keep temperature fixed and vary the thickness/disorder of the films. AHE measurements in ultra-thin  $\text{CNi}_3$  films are presented as a function of sheet resistance in the range of  $R_Q/100$  to  $R_Q$  at a constant temperature of 2 K. In addition, tunneling DOS spectroscopy is used to measure both the strength of the  $e$ - $e$  correlation effects and the electron polarization in the films.

Thin films of the metastable intermetallic  $\text{CNi}_3$  were deposited onto liquid nitrogen cooled, fire-polished glass substrates by electron-beam evaporation of  $\text{CNi}_3$  targets. Stencil masks were used to form either a Hall geometry (1.5 mm x 4.5 mm) or a film pattern more appropriate for planar tunneling measurements. The films formed a dense, homogenous C-Ni base which showed no sign of granularity down to the 1 nm scale using atomic force microscopy. Some carbon, in the form of multiwall carbon nanotubes, was precipitated out during the quench condensation of the vapor, but their density was too low to affect the transport [14]. Films in the thickness range of 2 to 10 nm were metallic in appearance, though partially transparent, and adhered extremely well to the glass substrates. Resistance and Hall measurements were made in Quantum Design PPMS using a standard four-wire dc I-V method. Probe currents of 1 mA and 1  $\mu$ A were used in Hall effect and transport measurements, respectively. The samples were vapor cooled down to 2 K in magnetic fields  $\pm 9$  T via the PPMS. The details of preparation of superconducting Al tunneling counter-electrodes on the films have been described elsewhere [15]. The tunneling data was taken in a dilution refrigerator equipped with an *in situ* mechanical rotator and a 9 T superconducting solenoid.

The lower inset of Fig. 1 shows the sheet resistance  $R$  of several  $\text{CNi}_3$  films of varying thickness as a function of  $\ln T$ . Though the 6 and 4 nm films exhibit metallic behavior at high temperatures, a logarithmic temperature dependence emerges at low  $T$ , as highlighted by the dashed lines in the inset. This behavior is a hallmark of two-dimensional weak-localization and is clearly evident below 20 K [1]. However, the film disorder increases rapidly with decreasing thickness (see Fig. 2 inset), and the resistance of the thinner films increases faster than  $\ln T$ . The upper inset in Fig. 1 is the tunnel junction conductance of three  $\text{CNi}_3$  films of varying thickness. These data were taken at 100 mK in a 7 T magnetic field oriented parallel to the film surface. The field was chosen to be above the parallel critical field

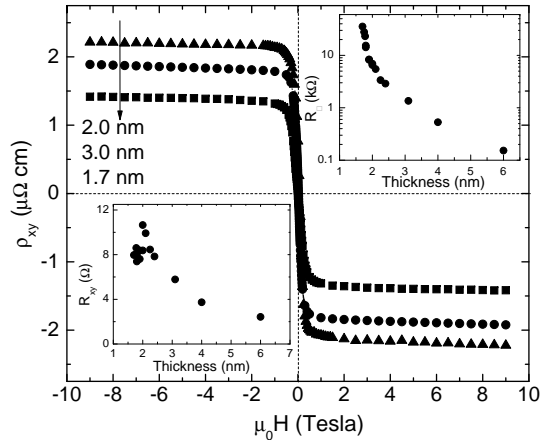


FIG. 2: The 2 K Hall resistivity of three films with the same thicknesses as those in the upper inset of Fig. 1. Upper inset:  $\text{CNi}_3$  sheet resistance as a function of film thickness at 2 K. Lower inset: Anomalous Hall resistance as a function of film thickness at 2 K.

of the Al counter-electrode, and, at this low temperature, the tunneling conductance was simply proportional to the DOS of the film [16]. The dip in the DOS spectrum at  $V = 0$  reflects the suppression of states near the Fermi energy as a result of  $e$ - $e$  interactions and is commonly referred to as the zero bias anomaly [2, 12]. In 2D the anomaly varies logarithmically with energy,  $\Delta G/G \sim \ln(V)$ , in the weak disorder limit. The 3 nm spectrum in the inset figure does, indeed, vary as  $\ln V$  and agrees well with that measured in thin Be films [12]. However, as the disorder is increased, the strength of the anomaly grows and eventually becomes algebraic in energy,  $\Delta G/G \sim V^\alpha$ . Deep in the strong localization limit,  $R \gg R_Q$ , the previously perturbative anomaly becomes a full-blown Coulomb gap with  $\alpha = 1$  [12]. In this regime the transport is expected to be of a modified variable range hopping form [17],

$$R(T) = R_0 \exp(T_0/T)^{1/2}, \quad (2)$$

where  $R_0$  is a constant of the order of  $h/2e^2$  and  $T_0$  is the correlation energy. The main panel of Fig. 1 shows a semi-log plot of sheet resistance as a function of  $T^{-1/2}$  for a 1.7 nm thick film, which is the thinnest used in this study. Fitting the data to Eq. 2 gives  $T_0 = 1.9$  K. Interestingly, the variable range hopping behavior extends to temperatures well above  $T_0$  [18] and is observed in a region where the Coulomb gap, as measured by tunneling, is not fully developed. Nevertheless, the tunneling data show a non-perturbative depletion of states in the thinnest films that is consistent with what has been reported in critically disordered Be films [12]. Given this clear signature of the onset of the correlated insulator regime, we now turn to the evolution of the AHE.

In Fig. 2 we plot the 2 K Hall resistivity,  $\rho_{xy} = R_c \mu_o M$ , as a function of applied perpendicular field for three  $\text{CNi}_3$  films of the same thicknesses as used in the upper inset of Fig. 1. The step-like structure at low fields ( $\mu_o H < 1$  T) represents the AHE, and the shallow-sloped higher field data represent the ordinary Hall effect. We note that, in the weak- to moderately-disordered regime, the magnitude of the anomalous Hall resistivity is expected to increase as a super-linear power of the sheet resistance  $\rho_{xy} \sim R^\beta$  [5, 6]. However, the data in Fig. 2 show that, in the thinnest films,  $\rho_{xy}$  is neither monotonic in film thickness nor sheet resistance.

In principle, the local maximum in  $\rho_{xy}$  could be a consequence of a thickness-dependent magnetization. A particular concern is that the magnitude of the magnetization is suppressed in films with  $t < 2$  nm, which, of course, would be reflected in a smaller AHE [8, 19]. To address this issue we have employed Tedrow and Meservy's spin polarized tunneling technique [20] to directly measure the electron polarization in the  $\text{CNi}_3$  films. The technique exploits the fact that, when a magnetic field is applied in the plane of a thin superconductor, in our case the Al counter-electrode, the BCS DOS spectrum is Zeeman-split into well resolved spin sub-bands. Figure 3 shows the normalized tunneling conductance vs. bias voltage of Al- $\text{AlO}_x$ - $\text{CNi}_3$  tunnel junctions on different thickness  $\text{CNi}_3$  films in a 4 T parallel magnetic field. The arrows denote the respective spin assignments of the occupied and unoccupied sub-band peaks. When tunneling into a paramagnetic metal the peaks are symmetrically positioned about  $V = 0$ . However, as is clearly evident in the figure, the peak heights are asymmetric, reflecting the unequal spin populations in the ferromagnetic

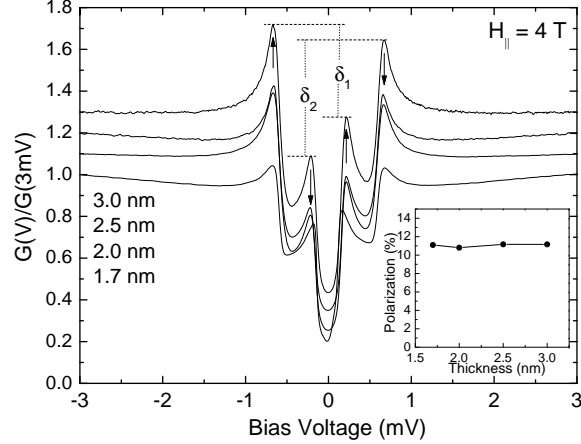


FIG. 3: The normalized tunneling conductance as a function of bias voltage for Al-AlO<sub>x</sub>-CNi<sub>3</sub> tunnel junctions on different thickness CNi<sub>3</sub> films in a 4 T parallel magnetic field at 100 mK. The curves have been shifted vertically for clarity. Inset: The corresponding polarizations of the 1.7, 2.0, 2.5 and 3.0 nm CNi<sub>3</sub> films.

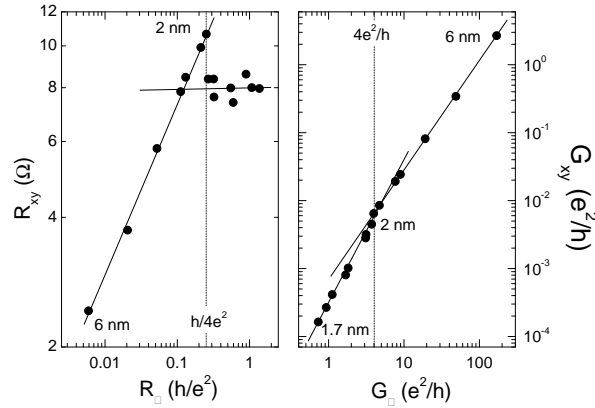


FIG. 4: Left panel: Log-log plot of the anomalous Hall resistance of CNi<sub>3</sub> films as a function of the sheet resistance at 2 K. The solid lines provide a guide to the eye. Right panel: Log-log plot of the anomalous Hall conductance as a function of the sheet conductance at 2 K. The solid lines represent separate power law fits to the low and high conductance data, giving exponents of  $\varphi = 2.0$  and 1.6, respectively.

CNi<sub>3</sub>. The electron polarization  $P$  is obtained by measuring the relative heights of the peaks [15, 20],

$$P = \left| \frac{\delta_1 - \delta_2}{\delta_1 + \delta_2} \right|, \quad (3)$$

where the peak height differences  $\delta_1$  and  $\delta_2$  are defined in Fig. 3. The electron polarization of the CNi<sub>3</sub> films with different thickness were are all about 11%. In the inset of Fig. 3 we plot  $P$  as a function of film thickness. Although polarization is not equivalent to magnetization, direct measurements of  $P$  in a variety of Ni alloys [21] has shown that the  $P$  accurately tracks the saturation magnetization across a wide range in  $M$ . Thus the data in Fig. 3 strongly suggest that the magnetization of CNi<sub>3</sub> films remains unchanged in the thickness range of 1.7 to 3 nm. Thus the non-monotonic behavior in Fig. 2 is due to quantum corrections to the anomalous Hall coefficient  $R_e$ .

The evolution of the AHE with increasing disorder is shown in the log-log plots of Fig. 4. Because of the 2D nature of the transport, we present the data in terms of longitudinal sheet resistances and conductances, along with the corresponding Hall resistances and conductances. In the left panel we show the anomalous Hall resistance as a

function of sheet resistance at 2 K. As expected  $R_{xy}$  initially increases with increasing  $R$ , but near  $R = h/(4e^2)$  the Hall resistance abruptly saturates. The saturation threshold occurs at a film thickness  $t \sim 2$  nm. In the right panel of Fig. 4 we plot the anomalous Hall conductance  $G_{xy} \approx R_{xy}/R^2$  as a function of the sheet conductance. Note that there is a kink in the curve near  $G = 4e^2/h$  where the scaling exponent changes from 1.6 to 2.0 as the film thickness is lowered below the 2 nm threshold. Recent numerical work on the AHE in ferromagnetic transition metals suggests that the Hall conductivity in the moderately disordered regime is dominated by intrinsic mechanisms [22–24] as opposed to extrinsic scattering processes that are prominent in very low disorder systems [5]. In the moderately disordered, weak localization regime of  $10^4$  S/cm  $\lesssim \sigma_{xx} \lesssim 10^6$  S/cm the AHE is dissipationless with  $\sigma_{xy} \sim R^0$ . However in the “dirty metal” regime,  $10^3$  S/cm  $\lesssim \sigma_{xx} \lesssim 10^4$  S/cm the Hall conductivity scales as  $\sigma_{xy} \sim R^\varphi$ , where  $\varphi$  ranges between 1.6 and 2.0, depending on the details of the calculation [23, 24]. We note that the low-temperature conductivity of our films varies from  $\sim 10^4$  S/cm to  $\sim 10^3$  S/cm in the thickness range of 6 to 2 nm. Thus, we believe that the data in the 2–6 nm range of Fig. 4 is, in fact, in the “dirty metal” regime, with a corresponding exponent  $\varphi = 1.6$ . This is in good agreement with what has been reported in a wide variety of itinerant ferromagnets of similar disorder [22, 25, 26]. The knee in the scaling plot probably reflects the fact that the films cross over from logarithmically localized transport to modified variable-range hopping transport in the vicinity of the quantum resistance. This crossover is, of course, commensurate with the rapid depletion of states near Fermi energy, see upper inset of Fig. 1, which is a precursor to the emergence of the Coulomb gap [12]. Recently Nagaosa *et al.* [5] have suggested that the low-temperature phase diagram of the AHE should include a phase boundary near the Mott-Anderson critical region. They estimate the zero-temperature boundary should be in the vicinity of  $\sigma = 10^3$   $\Omega^{-1}\text{cm}^{-1}$ , which roughly corresponds to the separatrix in the right panel of Fig. 4.

In summary, we show that the anomalous Hall resistance saturates in homogeneous  $\text{CNi}_3$  films with sheet resistance near the quantum resistance, although the electron polarization remains unchanged. We believe that the saturation is associated with the crossover from the weak localization regime to that of a 2D correlated insulator. The crossover is also clearly evident in the scaling behavior of the Hall conductivity as well as in the tunneling density of states.

We thank John DiTusa and Ilya Vekhter for enlightening discussions. This work was supported by the DOE under Grant No. DE-FG02-07ER46420.

- 
- [1] P. A. Lee and T. V. Ramakrishnan, *Rev. Mod. Phys.* **57**, 287-337 (1985).
  - [2] B. L. Altshuler, A. G. Aronov, M. E. Gershenson, and Yu. V. Sharvin, *Sov. Sci. Rev. A. Phys.* **9**, 223 (1987).
  - [3] D. B. Haviland, Y. Liu, and A. M. Goldman, *Phys. Rev. Lett.* **62**, 2180 (1989); A. E. White, R. C. Dynes, and J. P. Garno, *Phys. Rev. B* **33**, 3549 (1986).
  - [4] D. J. Bishop, R. C. Dynes, and D. C. Tsui, *Phys. Rev. B* **26**, 773 (1982).
  - [5] N. Nagaosa, J. Sinova, S. Onoda, A. H. MacDonald, and N. P. Ong, e-print arXiv:0904.4154.
  - [6] G. Bergmann and F. Ye, *Phys. Rev. Lett.* **67**, 735 (1991).
  - [7] C. M. Hurd, *The Hall Effect in Metals and Alloys* (Plenum Press, New York, 1972).
  - [8] G. Bergmann, *Phys. Rev. Lett.* **41**, 264 (1978).
  - [9] A. Langenfeld and P. Wölfle, *Phys. Rev. Lett.* **67**, 739 (1991).
  - [10] Y. K. Lin, T. R. Novet, D. C. Johnson, and J. M. Valles, Jr., *Phys. Rev. B* **53**, 4796 (1996).
  - [11] P. Mitra, R. Mitra, A. F. Hebard, K. A. Muttalib, and P. Wölfle, *Phys. Rev. Lett.* **99**, 046804 (2007).
  - [12] V. Yu. Butko, J. F. DiTusa, and P. W. Adams, *Phys. Rev. Lett.* **84**, 1543 (2000).
  - [13] For a review, see A.M. Goldman and N. Markovic, *Phys. Today* **51** (11), 39 (1998).
  - [14] D. P. Young, A. B. Karki, P. W. Adams, J. N. Ngunjiri, J. C. Garno, H. W. Zhu, B. Q. Wei, and D. Moldovan, *J. Appl. Phys.* **103**, 053503 (2008).
  - [15] Y. M. Xiong, P. W. Adams, and G. Catelani, *Phys. Rev. Lett.* **103**, 067009 (2009).
  - [16] M. Tinkham, *Introduction to Superconductivity* (McGraw-Hill, New York, 1996).
  - [17] B. I. Shklovskii and A. L. Efros, *Electronic Properties of Doped Semiconductors* (Springer, New York, 1984).
  - [18] Modified variable range hopping has also been observed at temperatures  $T > T_0$  in thin Be films and Au/Be bilayers, see Ref. [12], and Y.M. Xiong, A.B. Karki, D.P. Young, and P.W. Adams, *Phys. Rev. B* **79**, 020510(R) (2009), respectively.
  - [19] N. Kurzweil, E. Kogan, and A. Frydman, *Phys. Rev. Lett.* **102**, 096603 (2009).
  - [20] P. M. Tedrow and R. Meservey, *Phys. Rep.* **238**, 173 (1994).
  - [21] R. Meservey, D. Paraskevopoulos, and P.M. Tedrow, *Phys. Rev. Lett.* **37**, 858 (1976).
  - [22] S. Sangiao, L. Morellon, G. Simon, J. M. DeTeresa, J. A. Pardo, J. Arbiol, and M. R. Ibarra, *Phys. Rev. B* **79**, 014431 (2009).
  - [23] H. Kontani, T. Tanaka, and K. Yamada, *Phys. Rev. B* **75**, 184416 (2007).
  - [24] S. Onoda, N. Sugimoto, and N. Nagaosa, *Phys. Rev. B* **77**, 165103 (2008).
  - [25] A. Fernandez-Pacheco, J. M. DeTeresa, J. Orna, L. Morellon, P. A. Algarabel, J. A. Pardo, and M. R. Ibarra, *Phys. Rev. B* **77**, 100403(R) (2008).

- [26] T. Miyasato, N. Abe, T. Fujii, A. Asamitsu, S. Onoda, Y. Onose, N. Nagaosa, and Y. Tokura, Phys. Rev. Lett. **99**, 086602 (2007).